Influence of Slow Diffusing Species on Mixture Diffusion of Hexane Isomers in Silicalite: Characterization by a New Cyclic Method

Kader Lettat
IFP Energies nouvelles, Rond-point de l'échangeur de Solaize, Solaize 69360, France

Laboratoire Réactions et Génie des Procédés, CNRS-Nancy-University, ENSIC, 1 rue Grandville, Nancy F-54000, France

Elsa Jolimaitre
IFP Energies nouvelles, Rond-point de l'échangeur de Solaize, Solaize 69360, France

Mélaz Tayakout
IRCELYON, UMR 5256, CNRS/Université Lyon 1 2 Av. Albert Einstein, Villeurbanne F-69626, France

Daniel Tondeur
Laboratoire Réactions et Génie des Procédés, CNRS-Nancy-University, ENSIC, 1 rue Grandville, Nancy F-54000, France

DOI 10.1002/aic.12679
Published online June 8, 2011 in Wiley Online Library (wileyonlinelibrary.com).

The feasibility of mono- and di-branched paraffins separation on silicalite was evaluated by performing cyclic breakthrough experiments in liquid phase with mixtures of 2-methylpentane (2MP), 3-methylpentane (3MP), 2,3-dimethylbutane (23DMB), and 2,2-dimethylbutane (22DMB). For mixtures of the faster diffusing species (2MP, 3MP, and 23DMB), cyclic steady state is obtained from the first cycle. On the other hand, when the slow diffusing species 22DMB is involved, a slow accumulation occurs from cycle to cycle, yielding a change of the breakthrough curves for all the species. Using a diffusion model especially adapted to adsorbent saturation loading, the kinetic and thermodynamic parameters of 22DMB were estimated. Influence of the cycling conditions on the separation performance were finally studied by simulation. © 2011 American Institute of Chemical Engineers *AIChE J,* 58: 1447–1455, 2012
Keywords: adsorption, liquid phase, diffusion, mixtures, zeolites, cyclic method

Introduction

Separation of multi-branched paraffins from single-branched paraffins is of great industrial interest, because of its potential applications in the enhancement of the octane number of fuel products. At low adsorption loading, it is now well known that the di-branched and the mono-branched isomers present strong diffusional differences in silicalite.[1–4] However, very few studies have been carried out in conditions more appropriate for an industrial separation, i.e., close to saturation loading. Still, experimental[4,5] and simulation[6] studies have shown that even at saturation loading, the apparent diffusion kinetics of the different isomers is strongly impacted by the presence of the other species. An additional important feature is that there may be species with very different diffusion kinetics. This situation

Correspondence concerning this article should be addressed to E. Jolimaitre at elsa.jolimaitre@ifpenergiesnouvelles.fr.

calls for specific approaches to modeling, parameter estimation, and process optimization, which the present work proposes to develop and illustrate.

To describe and predict the chromatographic behavior of such mixtures, it is necessary to have available:

- an adsorption and diffusion model that is able to represent this kind of behavior,
- an appropriate experimental methodology, so as to extract the associated parameters.

In a previous article,[7] a new model was proposed, based on the Maxwell-Stefan theory and specifically adapted to the case of solid saturation. Using this model, the 3-methylpentane, 2-methylpentane, and 2,3-dimethylbutane diffusivities have been estimated from classical breakthrough curves of adsorption from the liquid phase. However, the 2,2-dimethylbutane diffusivity could not be estimated, because the quantity of 22DMB that enters the solid during one single breakthrough experiment is too small.

In this article, an alternative method is proposed to retrieve the adsorption parameters of this species, which consists in accumulating 22DMB in the solid by performing successive adsorption/desorption steps. The slow accumulation of 22DMB in the zeolite pores yields a modification of the breakthrough curves of all species during the cycles. In this way, the 22DMB thermodynamic and kinetic parameters can be estimated, and the potentiality of the separation can be evaluated. We shall also illustrate that the experimental conditions required for parameter estimation may be quite different from that required to achieve a good separation.

Experimental Methods

Adsorbent characterization

The silicalite crystals used in this study were supplied by Zeolist International. The Si/Al ratio, measured by X-ray fluorescence, is 500% ± 50% (experimental uncertainties are important for such a high ratio). The few H^+ cations initially present in the zeolite framework were replaced by Na^+ cations using the conventional ion exchange technique and subsequent washing. Scanning electron microscopy showed that the crystals are spherical with a mean crystal radius of $R_c = 0.75 \times 10^{-6}$ m.

This zeolite was pelletized with a silica binder in IFPEN, then cut and sieved. Resulting pellets are small cylinders with a diameter of 0.85 mm and a mean length of 0.8 mm. For model simplification, particles were supposed to be spherical with a mean radius of $R_p = 0.41 \times 10^{-3}$ m. The binder mass ratio, determined from *n*-hexane adsorption gravimetric uptake experiments performed with both crystals and pellets, is 20%. In the rest of this article, the values of all the thermodynamic parameters are always corrected for the binder ratio. The porosity of the particles was measured by mercury porosimetry ($\varepsilon_p = 0.34$). Before experiments, the sample is activated in a nitrogen stream for 3 h at 300°C.

Experimental setup

Breakthrough and cyclic experiments were carried out according to standard procedures. The dynamic adsorption unit is described in our previous article.[7] A stainless steel column ($L_{bed} = 1$ m and $S = 0.848 \times 10^{-4}$ m^2) is packed with a known mass of pellets and placed into the oven. The interstitial porosity is calculated from the mass and the density of the pellets, giving $\varepsilon_i = 0.29$. During the experiment, the whole column is maintained at 35 bar and 185°C. Before the beginning of the cyclic experiment, the column is filled slowly (to avoid exothermicity problems) with the so-called solvent (or desorbent).

The cyclic experiments are quite simple to operate. The charge and the desorbent are successively injected at the bottom of the column for the selected adsorption and desorption times (t_{ads} and t_{des}), using an automatic valve connected to a computer. The desorbent is 2MP in all experiments, whereas the charge is composed of different mixtures of 3MP, 23DMB, and 22DMB. The liquid fractions of the effluent are collected and analyzed by a gas chromatograph with a FID detector and a PONA analytical column. The chromatograph and the automatic valve are run by the same automaton, so as to synchronize the valve and the samples collector. The number of samples collected for each cycle can vary as defined by the operator. For high numbers of cycles, only a few samples were collected for some of the cycles, to reduce the duration of the analysis.

The adsorbates are 2-methylpentane (2MP) and 3-methylpentane (3MP) purchased from Fluka Chemika, 2,3-dimethylbutane (23DMB) and 2,2-dimethylbutane (22DMB) purchased from SAFC. The specified purities are over 99%. All these adsorbates were used without further purification.

Model

Model equations

The model used in this study is the same as the one presented in a previous article[7] to which we refer the reader. Thus only some essential features are recalled here.

- At the macroscale, the column is represented by a cascade of 150 isothermal stirred tank reactors that account for both axial dispersion and dead volumes at the column inlet and outlet. The variation of the fluid velocity (due to adsorption and to the different molar volumes of the molecules) is taken into account.
- At the mesoscale, mass transfer resistances at the pellet surface and in the macropores are lumped into a single external film mass transfer coefficient k^m; an additional large mass transfer coefficient k^c, corresponding to a stagnant film around the zeolite crystals is also introduced, for performance of the numerical scheme uniquely; convection inside the macropores, due to differences in volume flow entering and leaving the adsorbent, is taken into account.
- At the microscale, that of the zeolite crystals, the transport phenomena are viewed as a compound of local thermodynamic equilibrium, of Dusty-Gas-Maxwell-Stefan type diffusion with negligible non-diagonal elements, and of volume constraints, rendered consistent by the Gibbs-Duhem constraints. These microscale aspects are discussed more in detail below.

The internal transport model used in the previous and present article is comparable to the well known model published by Krishna in 1990.[8] However, several modifications are introduced, the reasons and consequences of which were clarified in the previous article[7] and in subsequent discussions with Krishna and Van Baten.[9,10]

Table 1. Experimental Conditions for the Different Runs

Run	Feed (Mass %)	Desorbent	Flow-Rate (cc/min)	Cycle Conditions (tads/tdes) (min)	Number of Cycles
1	3MP	2MP	10	15/15	3
2	23DMB/3MP (50/50)	2MP	10	15/15	8
3	22DMB/3MP (50/50)	2MP	10	15/15	8
4	22DMB/3MP (70/30)	2MP	10	15/15	8
5	22DMB/3MP (85/15)	2MP	10	15/15	6
6	22DMB/3MP (85/15)	2MP	10	15/10	15
7	22DMB/3MP (85/15)	2MP	10	15/5	20
8	22DMB/3MP (85/15)	2MP	5	30/30	4

• Volume constraints are introduced in the microporosity (zeolite pores). The adsorbed phase molar volumes are supposed to be the same as in the fluid phase for all molecules. Consequently, the solid is not represented by vacant sites but by the residual adsorbent volume (the volume which is not occupied by the adsorbed molecules). Moreover, the force exerted on species i due to the friction with the solid is taken as proportional to the volume fraction (instead of the molar fraction) of solid.

• The reference for the diffusion fluxes in the microporosity is the barycentre of the volume of all species, including the solid matrix. Consequently, the flux corresponding to the solid is not set to zero, but instead is taken as a variable.

• The state variable for the adsorbed phase is the fictitious fluid in equilibrium with the adsorbed phase. It has been shown[11] that this change of variable makes the system of equations more compact.

The size of the diffusing molecules being very close to the pore diameter, we also assumed that there is no counter-diffusion between the adsorbed species i and j inside single pores (diffusion with no mutual interaction), which leads to canceling the non-diagonal elements in the Maxwell-Stefan matrix. This restrictive assumption is criticized by Krishna and van Baten[9,12] who advocate that the effect of the exchange coefficients D_{ij} becomes dominant at saturation. In our case, introduction of the exchange coefficients was not necessary to correctly represent the behavior of the system.[10] We believe that there are two reasons for that. First, because in our model the coupling of the transport equations of the different species at the microscopic level is taken into account via the thermodynamic equilibrium relations, the volume constraints and the non-zero solid flux. Such constraints are absent in Krishna and van Baten's approach, which therefore requires non-diagonal elements to express the cross-effects. Second, because the C_6 molecules used in our experiments are much larger than the molecules studied by Krishna and van Baten[12] and the hypothesis that there is no counter-diffusion between the adsorbed species is more appropriate in this case. The final set of equations, based on the assumptions detailed above, can be found in details in our previous article.[7]

Cyclic simulations

Cyclic simulations were performed by applying cyclic boundary conditions on the fluid phase equations. Note that the charge and the desorbent are both injected at the bottom of the column (circulation in the column is always upflow). Consequently, only the boundary conditions at the bottom of the column are cyclically changed.

For $n = 1,n_{\text{cycles}}$:

adsorption steps: $(n-1)\cdot t_{\text{cycle}} < t < (n-1)\cdot t_{\text{cycle}} + t_{ads}$

$\phi_j^{f,0} = \phi_j^{f,ads}$

desorption steps: $(n-1)\cdot t_{\text{cycle}} + t_{ads} < t < n\cdot t_{\text{cycle}}$

$\phi_j^{f,0} = \phi_j^{f,des}$

with $t_{\text{cycle}} = t_{ads} + t_{des}$

A summary of all the runs with the corresponding experimental conditions can be found in Table 1.

Fixed parameters

All the parameters relative to the physical characteristics of the adsorbent, the geometry of the columns, and the external mass transfer parameters have been determined independently and can be found in our previous article.[7] The mass transfer coefficients at the surface of the crystals k^c is always chosen large so that the corresponding transfer resistance is negligible. The lumped macroporous mass transfer coefficient k^m was calculated using (the fluid film around the pellet is neglected):

$$k^m = \frac{5.\varepsilon_p.D^{mac}}{R_p}$$

with $D^{mac} = \frac{D_m}{\tau}$ where D_m is the molecular diffusion coefficient, considered the same for all components since the molecules are very similar ($D_m = 2.2\cdot 10^{-8}\ m^2/s$) and τ is the tortuosity factor, fixed at a value of 3.8.

This finally gives $k^m = 2.4\cdot 10^{-5}\ m/s$.

Finally, the Langmuir parameters and diffusivities of 3MP, 2MP, and 23DMB species are given in Table 2. These parameters are directly retrieved from our previous article.[7]

Estimated parameters

The kinetic and thermodynamic estimated parameters in this work are related to the 22DMB species. Since the system is at (or near) saturation, the Langmuir law can be reduced by considering that $\sum_{j=1}^{nc} b_j C_j >> 1$, the only independent estimable parameters are:

• the ratio of the Langmuir coefficients b_j/b_1 $j = 2,nc$

• the Maxwell-Stefan diffusion coefficients $D_{j,nc+1}$ $j = 1,nc$

Only co-adsorption isotherms and Maxwell-Stefan diffusion coefficient can be estimated from liquid phase breakthrough curves. Therefore, only the 22DMB Langmuir coefficients ratio (relative to 2MP) and 22DMB diffusion coefficient will be evaluated.

Table 2. Langmuir Parameters and Diffusivities for Each Species

	3MP	2MP	23DMB	22DMB
q_j^{sat} (mol/m^3)	1500	1650	1200	1200
q_j^{sat} (molecule per unit cell)	4.8	5.3	3.8	3.8
b_j/b_{2MP} (-)	1.0	–	0.55	0.5
$D_{j,nc+1}$ ($m^2 \cdot s^{-1}$)	3.6×10^{-15}	2.1×10^{-15}	6.1×10^{-16}	10^{-17}
$D_{j,nc+1}/D_{3MP,nc+1}$	1	1.7	5.9	360
$D_{j,nc+1}/D_{3MP,nc+1}$ from Cavalcante and Ruthven[1]	1	0.6	43	780

For 3MP, 2MP, and 23DMB: Parameters estimated using simple breakthrough curves in a previous study.[7]
For 22DMB: Parameters estimated using this study's cyclic experiments.

Numerical solution of model equations

The set of partial differential equations is first reduced to a set of ordinary differential equations by applying an orthogonal collocation technique to the spatial coordinate corresponding to the crystal radius, using the subroutines JCOBI and DFOPR developed by Villadsen and Michelsen.[13] Axial dispersion along the bed length is represented by the series of CSTR. The resulting ordinary differential-algebraic system of equations is solved using the DDASPG integration subroutine (IMSL library), based on the Petzold-Gear BDF method.

The parameters are grouped in the parameters vector. The optimization is performed by a Levenberg-Marquard procedure (subroutine DBCLSF of the IMSL library).

Results and Discussion

A complete set of cyclic experiments were measured using the above described experimental set-up.

When only the fastest diffusion species are present (2MP, 3MP, and 23DMB), no accumulation was observed during the cycles, and the cyclic steady-state is reached immediately from the first cycle. Thus, cyclic experiments can be simulated using diffusivities estimated from classical breakthrough experiments, as described previously.[7] When 22DMB is present, however, this procedure does not apply, because of insufficient penetration of this species into the zeolite, and therefore insufficient sensitivity of the experiments to the parameters of this species. Indeed, a very slow accumulation of this molecule inside the zeolite porosity occurs from cycle to cycle. Under appropriate experimental conditions, this accumulation has a cumulative influence on the breakthrough curves of the faster species, which evolve noticeably as the cycles are carried on. It then becomes possible to estimate the thermodynamic and kinetic parameters of 22DMB from these cyclic experiments. These results will now be developed in more details. The final set of estimated parameters can be found in Table 2.

3MP/2MP cyclic experiments

The first experiment was performed with fast-diffusing species. The charge is composed of pure 3MP and the desorbent is pure 2MP (run 1). The results can be seen on Figure 1a. The cycles are impossible to tell apart, and this is even more obvious when the first and last cycles are superimposed (Figure 1b). No accumulation of the monobranched isomers is detected during the cycles: 3MP is entirely desorbed at the end of the desorption step. These results also show the very good reproducibility that can be obtained with the experimental device.

A simulation of the whole cyclic experiment was performed using the model described above and the thermodynamic and kinetic parameters estimated from simple breakthrough curves (Table 2). The simulation is in very good agreement with the experimental results.

(3MP+23DMB) versus 2MP cyclic experiments

Even though diffusion of 23DMB in silicalite is much slower than that of the monobranched isomers (the diffusion coefficient is smaller by almost an order of magnitude, see Table 2) the cyclic experiment with a 50/50 mixture of 23DMB and 3MP (run 2) does not show any evolution of the breakthrough curves from cycle to cycle, as can be seen on Figures 2a, b. The adsorbent is totally regenerated at the end of each desorption step.

This behavior is correctly predicted by the parameters estimated from simple breakthrough curves, even though the agreement between the experimental and simulated cycles is not as good as for the 2MP/3MP mixtures. As observed in our previous work,[7] the shapes of the ternary breakthrough curves involving 23DMB seem to indicate an inversion of the apparent selectivity. For binary systems, the 3MP/2MP exchange isotherm is linear, whereas the 23DMB/2MP

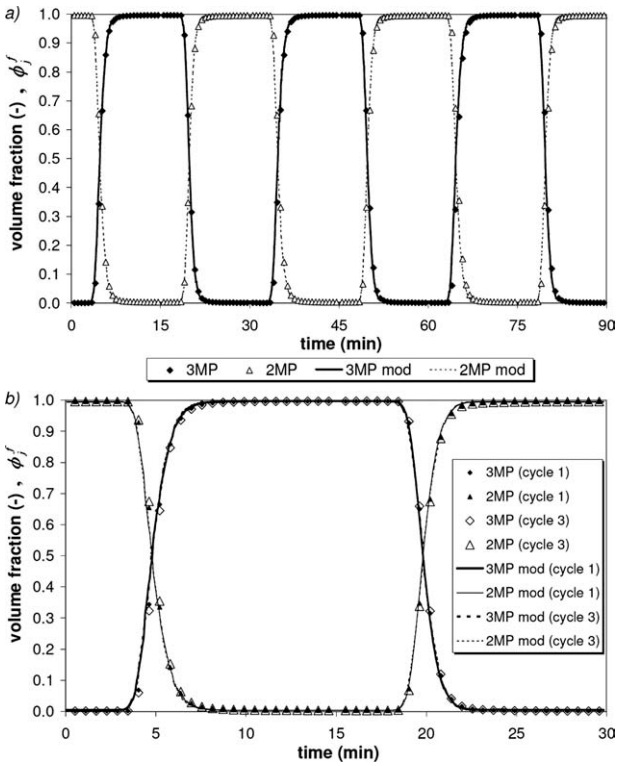

Figure 1. 3MP/2MP cyclic experiment and modeling (run 1) (a: all the cycles; b: superposition of first and last cycle).

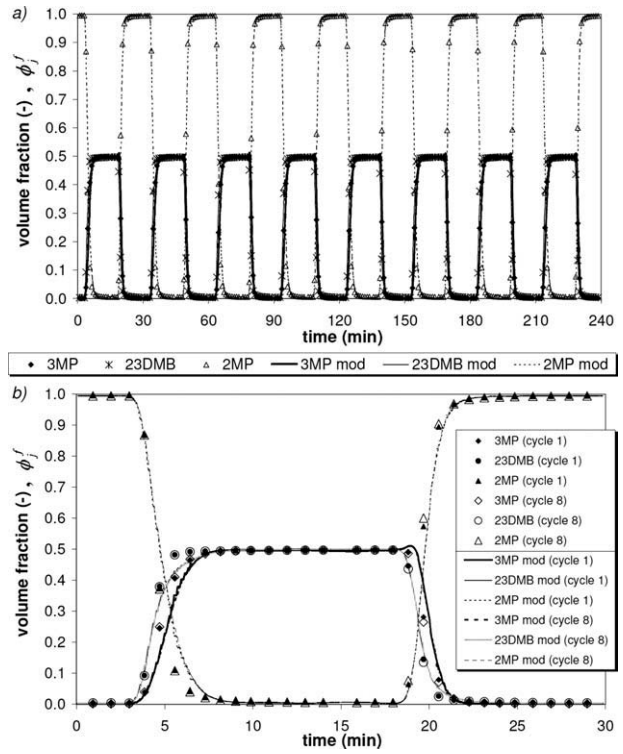

Figure 2. 3MP+23DMB/2MP cyclic experiment and modeling (run 2) (a: all the cycles; b: superposition of first and last cycle).

exchange isotherm is favorable to 2MP. In the ternary 3MP+23DMB/2MP system, the 23DMB and 2MP breakthrough and inverse breakthrough curves can be perfectly superimposed, which is a characteristic of linear exchange isotherms. On the contrary, the 3MP adsorption front is relatively spread out whereas its reverse, the desorption front is steeper. This phenomenon can be explained either by an inversion of the thermodynamic selectivity or by a complex diffusion behavior not represented by our model. Nevertheless, the complete regeneration of the solid is predicted by the simulations, showing that 23DMB diffuses slower than 2MP and 3MP, but is still reasonably fast. Consequently:

- the quantity of 23DMB that adsorbs in silicalite during one single breakthrough curve is significant, making it possible to estimate the 23DMB diffusivity from one single breakthrough curve,
- 23DMB is totally desorbed from silicalite at the end of each desorption step.

It is important to note that these conclusions are dependent on the experimental conditions chosen. It is probable that for higher flow rates or lower cycle times, an evolution of the breakthrough curves with cycle number would be visible. This point is discussed in more detail below, along with the results obtained with 22DMB.

(3MP+22DMB) versus 2MP cyclic experiments

These experiments now involve the so-called slow species 22DMB in mixture with the fast species 3MP, and with 2MP as the desorbent; and we shall give these experiments a more detailed attention.

Influence of 22DMB Concentration Figure 3 shows 3MP breakthrough curves for both the adsorption and the desorption step, for three different runs corresponding to three different charge composition (the other species are not represented for more legibility). The breakthrough curves of cycles 1 and 6 are superimposed through a proper shift of the time scale. As opposed to the previous experiments, a shift of the 3MP breakthrough curves is visible when 22DMB is present in the charge.

For the 50/50 mixture, the shift is very small. Only a slight decrease of the 3MP first moment for the last cycle can be detected, indicating that the quantity of monobranched isomers adsorbed (and therefore desorbed) decreases with cycles.

For higher 22DMB concentrations, the difference between the cycles is amplified, as well as the roll-over of 3MP during desorption, because the quantity of 22DMB adsorbed in silicalite during the adsorption step is more important:

- the thermodynamic equilibrium is more in favor of 22DMB,
- the 22DMB diffusion driving force is higher.

Still, the shift of the breakthrough curves during the cycles is not sensitive enough to enable satisfactory 22DMB parameters estimation. It was therefore decided to amplify the phenomenon by changing the desorption step duration.

Influence of the Desorption Time Three runs (5, 6, and 7) were performed with a 22DMB rich mixture (85%), keeping the same adsorption time (15 min) but with different

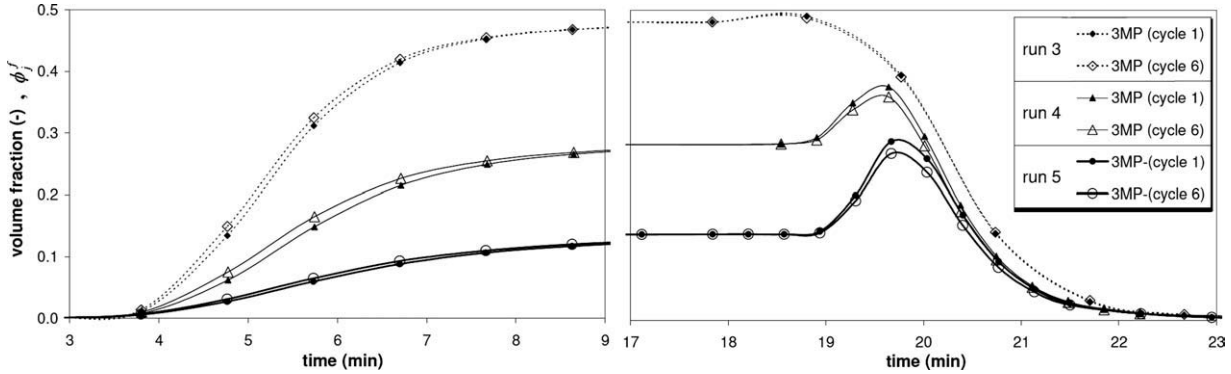

Figure 3. 3MP+22DMB/2MP cyclic experiments for different 3MP/22DMB feed mass fraction (run 3: 50/50, 4: 30/70, and 5: 15/85): superposition of cycles 1 and 6.

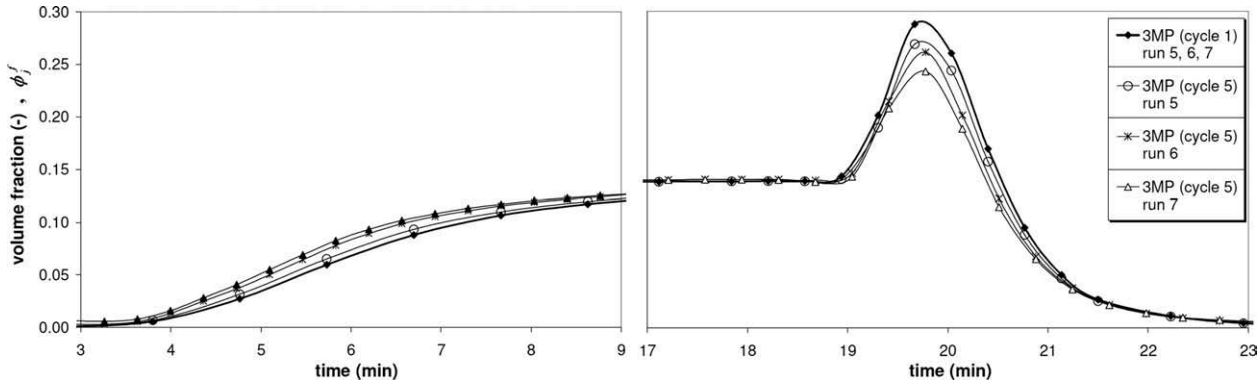

Figure 4. 3MP+22DMB/2MP cyclic experiments for different desorption times (run 5: t_{des}=15 min; run 6: t_{des}=10 min, run 7: t_{des} = 5 min): superposition of Cycles 1 and 5.

desorption times (15, 10, and 5 min). The results, displayed as 3MP breakthrough curves on Figure 4, show that for lower desorption times, accumulation of 22DMB in the adsorbent at each cycle is more important: the shift of the monobranched isomer breakthrough curves is clearly amplified. This effect is particularly visible on the amplitude of the 3MP roll-up during the desorption step. As 22DMB accumulates in the adsorbent, the available pore volume for 3MP diminishes. The quantity of 3MP adsorbed and desorbed in each cycle becomes smaller and smaller, and the amplitude of the 3MP roll-up drops significantly. Note that, to obtain superimposition of the curves, the time scale on Figure 4 does not correspond to the absolute experimental time but to the adsorption (or desorption) step time. Since the 3MP roll-up is very sensitive to 22DMB accumulation, the 22DMB diffusivity can be estimated from these cyclic experiments.

22DMB Parameters Estimation. The estimation procedure consists in finding the 22DMB parameters that minimize the difference between the experimental and simulated cyclic breakthrough curves (all the cycles are taken into account). Estimation was performed on run 7. The criterion to minimize with respect to both the Langmuir ratio $\left(b_{22DMB}/b_{2MP}\right)$ and the Maxwell-Stefan diffusivity of 22DMB is the sum of the square difference between the experimental results and the simulated ones under the physical constraint that parameters are non negative. The saturation concentration $q_{22DMBsat}$ was fixed at the same value as that of 23DMB, i.e., 3.8 mol/u.c. Indeed, the 22DMB saturation concentration can not be measured experimentally in our operating conditions, because the minute penetration of this molecule prevents from making consistent mass balances on the breakthrough curves. The equivalence between 22DMB and 23DMB saturation concentration is coherent with the theoretical value of four molecules per cell, corresponding to the channel intersection sites, and is confirmed by literature results.[1,14]

The estimated parameters can be found in Table 2. The comparison between experiment and simulation is plotted in Figure 5. It appears that the evolution of the 3MP roll-up with time can be correctly represented with a 22DMB diffusivity of 10^{-17} m^2/s, i.e., about 60 times smaller than the 23DMB diffusivity. This is not very surprising, since the experimental results for the two molecules are quite different (no cyclic accumulation of 23DMB, non negligible quantity of 23DMB adsorbed during a single breakthrough curve). On the contrary, the 22DMB Langmuir coefficients ratio is very close to that of 23DMB (0.5 vs. 0.55), confirming that the different behaviors cannot be explained by thermodynamic considerations.

The diffusivities ratios $D_{j,nc+1}/D_{3MP,nc+1}$ obtained from this work are compared to those obtained by Cavalcante and Ruthven[1] in Table 2. The trends are globally equivalent: 2MP and 3MP have very close diffusion coefficients, 22DMB is slower by several orders of magnitude, and 23DMB is located in between. The quantitative differences can be explained by the different experimental conditions (pure component gas phase experiments at low loadings in the case of Cavalcante and Ruthven vs. liquid phase mixtures experiments at saturation, in our case).

Nonetheless, the shape of the 3MP breakthrough curves is not very accurately simulated by the model (Figure 6). Breakthrough occurs later for the simulations, and the simulated plateau at the end of the adsorption step is higher than the experimental one.

It is important to realize that when parameter estimation is carried out only on the first cycle, it is possible to fit one single breakthrough curve better with a 22DMB diffusivity in the same order of magnitude as that of the monobranched isomers. However, simulating the whole cyclic experiment with this diffusivity yields no evolution whatsoever from

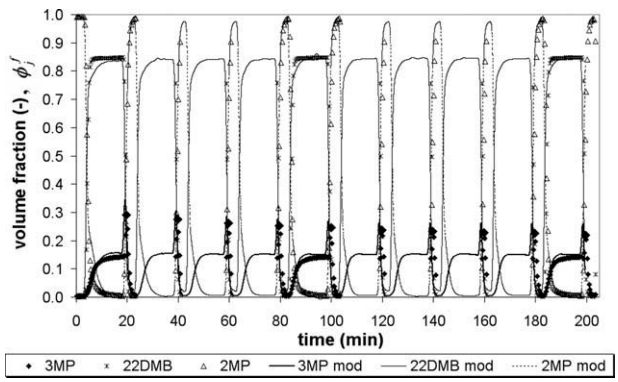

Figure 5. 3MP+22DMB/2MP cyclic experiments and modeling for run 7.

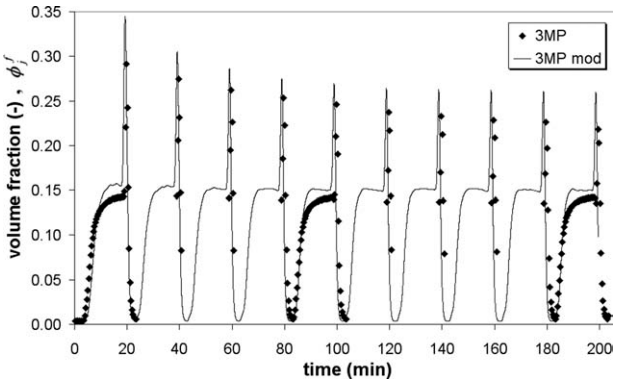

Figure 6. 3MP+22DMB/2MP cyclic experiments and modeling for run 7: zoom on the 3MP breakthrough curve.

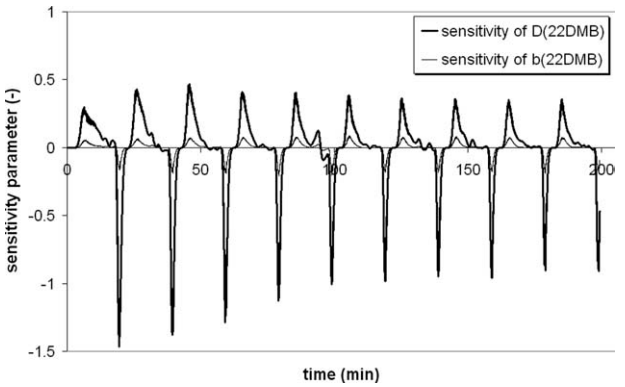

Figure 7. D_{22DMB} and b_{22DMB} sensitivity for run 7.

cycle to cycle, and thus cannot represent, even qualitatively, the full experimental behavior. The corresponding 22DMB diffusivity has no physical meaning.

To summarize, we were not able to obtain simultaneously a good fit of the breakthrough curve shape and of its evolution from cycle to cycle. This points out an intrinsic limitations of the model. It is probable that some of the hypotheses are not verified. For example, the generalized Langmuir model may not be totally appropriate. It has been shown in the literature[15,16] that mixture adsorption of normal alkanes in silicalite cannot be represented by a Langmuir model: because of very complex molecular packing effects, the binary adsorption isotherms show non-ideal behaviors, such as selectivity reversals. The same detailed measurements are not available for mixtures of mono- and di-branched isomers, but it is probable that these systems are also characterized by very complex adsorption thermodynamics. This hypothesis is also supported by the unexpected behavior of the 3MP/2MP/23DMB system as discussed above.

Another possibility is that the binary exchange diffusion coefficient D_{ij} may not be left aside.

With this in mind, a parameter sensitivity study has been carried out, by calculating the influence of a variation of the estimated parameters on the model output. A parameter P_i is experimentally identifiable if (1) its sensitivity is not negligible $\frac{\partial M(t)}{\partial P_i} \neq 0$ and (2) its sensitivity is not proportional to the sensitivity of any other parameter $\frac{\partial M(t)}{\partial P_i} \neq A \cdot \frac{\partial M(t)}{\partial P_k} \quad \forall k \neq i$, where $M(t)$ is the output of the model and A a constant (independent of time). The sensitivity of the 22DMB parameters (diffusivity and Langmuir coefficient) on the 3MP breakthrough curves are shown in Figure 7. The sensitivity is calculated using the formula $\frac{M(t)|_{Pi} - M(t)|_{Pi+\Delta Pi}}{\Delta P_i / P_i}$ and is therefore dimensionless. As expected, both parameters are sensitive, i.e., have a clear influence on the 3MP outlet concentration. The sensitivities show two maxima: one corresponding to the 3MP breakthrough time (adsorption step) and the other to the 3MP roll-up (desorption step), that is to say the positions of the breakthrough curves where the concentrations vary the most. For a given cycle, the sensitivities of the two parameters have roughly the same shape, i.e., they are nearly proportional. It is therefore not possible to dissociate the effects of the thermodynamic and kinetic parameter from one single cycle. On the other hand, the sensitivity of the Maxwell-Stefan diffusivity varies with cycles, which is not the case for the Langmuir coefficient. This confirms once again that in order to be valid, the parameter estimation procedure has to be applied to a whole cyclic experiment showing some evolution with cycle number.

The simulated 22DMB adsorbed phase concentration at the bed outlet (averaged over the crystal radius) is plotted on Figure 8 as a function of time. At each cycle, 22DMB accumulates in the adsorbent, until it reaches a cyclic steady state. At the same time, the adsorbed 3MP quantity drops significantly. The adsorption of 22DMB is therefore greatly detrimental to the 3MP/22DMB selectivity and by extension to the quality of the 3MP/22DMB separation (since 3MP is the species that has to be selectivity retained in the adsorbent column).

Model Validation. Cyclic breakthrough curves at different experimental conditions (mixture concentration, adsorption and desorption times, flow rates) have been simulated using the estimated values of the isotherms and diffusion coefficients given in Table 2. The trends are respected for all the experiments, even though the amplitude of the 3MP roll-up is not always perfectly fitted (see the simulation of run 5 in Figure 9).

Influence of Cyclic Conditions on the Performance of Separation. Suppose we were to separate 22DMB from 3MP. To optimize this separation, it is interesting to study the effect of the cyclic conditions on the 22DMB and 3MP delta loadings. The delta loading is defined as the difference in

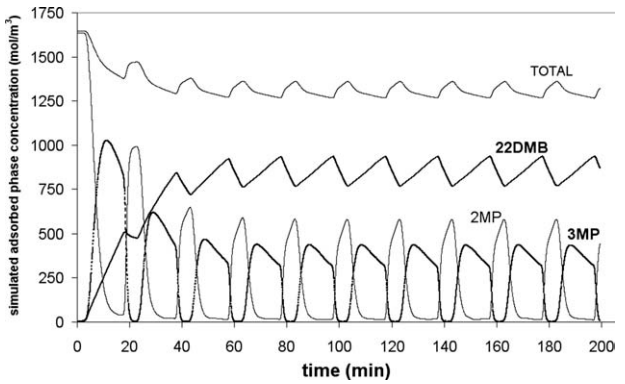

Figure 8. Simulated adsorbed phase concentration for run 7.

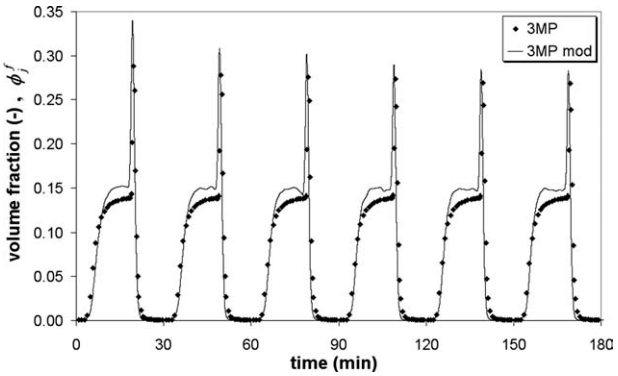

Figure 9. 3MP+22DMB/2MP cyclic experiments and simulation for run 5 (only 3MP shown for clarity).

adsorbent loading between the adsorption and desorption steps. The 3MP delta loading is directly proportional to the mass of adsorbent needed for the separation, (because the monobranched species are the ones which have to be selectivity adsorbed) that is to say the productivity, and has to be maximized. The 3MP/22DMB delta loading ratio is related to the separation selectivity and must also be as high as possible.

At a given mixture concentration, simulations have been performed for different adsorption/desorption times and for different flow rates, and the 22DMB and 3MP delta loadings have been calculated for each simulation. The results are presented in Table 3 and the mean simulated adsorbed concentrations (the average concentration in the crystals at the column outlet) for different adsorption/desorption times are illustrated on Figure 10. The delta loadings of both species increase with flow rate. Indeed, at higher flow rates, i.e., for lower adsorbate/adsorbent contact time, the cycle time being constant, the column is closer to complete breakthrough at the end of the adsorption step for the two molecules. Also, the 3MP/22DMB delta loading ratio increases, because 22DMB diffusion inside the zeolite is hindered. Thus, as expected, the kinetic separation is favored at higher flow rates (as long as the 3MP diffusion is not limiting).

For the same adsorption time, a lower desorption time yields logically a smaller delta loading for the two species. However, 22DMB is more affected, because of its diffusional limitation. Consequently, the 3MP/22DMB delta loading ratio is higher at lower desorption time. Lowering adsorption time also has a positive effect on selectivity, but induces a drastic drop in 3MP delta loading.

Finally, the best separation conditions are logically obtained at high flow rates and high desorption times. Under these conditions, the quantity of 22DMB adsorbed in silicalite is small

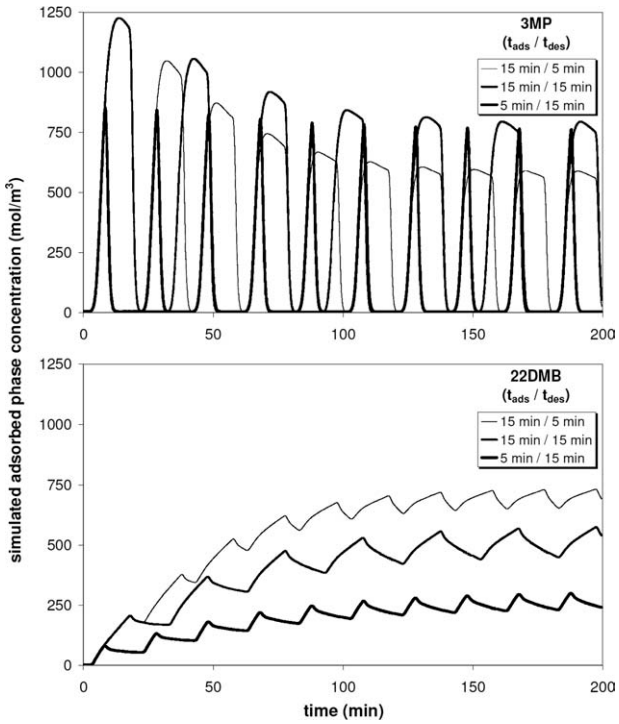

Figure 10. Simulated adsorbed phase concentration for 3MP and 22DMB for different adsorption/desorption times.

and the 3MP/22DMB delta loading ratio is large. One gets closer to the "ideal" situation where the "slow" species would not be adsorbed at all. It is interesting to note that the conclusions are totally opposite when one wishes to estimate 22DMB diffusivity from cyclic experiments: the quantity of 22DMB adsorbed has to be important, so as to amplify its effect on the faster isomers breakthrough curves.

Conclusion

Diffusion of mono- and di-branched paraffins in silicalite was studied by a cyclic chromatographic method in the liquid phase, that is to say near the adsorbent saturation loading.

For the faster diffusing species (2-methylpentane, 3-methylpentane, 2,3-dimethylbutane) all the cycles are identical: the first cycle is sufficient to estimate the diffusivity and equilibrium parameter of these molecules. When 2,2-dimethylbutane is present however, the quantity adsorbed during the first cycle is very small, and a very slow accumulation is observed during the next cycles.

Table 3. Effect of Cyclic Conditions on 3MP and 22DMB Delta Loadings

Flow Rate (cc/min)	Adsorption Time (min)	Desorption Time (min)	3MP Delta Loading (mol/u.c.)	22DMB Delta Loading (mol/u.c.)	3MP/22DMB Delta Loading Ratio
10	15	5	1.85	0.21	9.0
10	15	15	2.45	0.38	6.5
2	5	15	0.69	0.07	9.9
5	5	15	1.51	0.14	10.8
10	5	15	2.39	0.17	14.2
15	5	15	2.88	0.21	13.6

The influence of this slow accumulation on the breakthrough curves of the fast diffusing 3MP, when amplified by a proper choice of experimental conditions, allows to estimate the 22DMB kinetic and thermodynamic parameters. To do so, a model based on a modified Maxwell-Stefan approach and adapted to the special case of saturation loading was used. The model enables to correctly represent the evolution from cycle to cycle, but not the precise shape of the breakthrough curve: the Langmuir model is probably too basic to correctly characterize the complex adsorption of branched alkane mixtures in silicalite. The 22DMB Maxwell-Stefan diffusivity is nearly 2 orders of magnitude below that of 3MP and 2MP and 60 times smaller than that of 23DMB. The 22DMB Langmuir coefficient is two times smaller than that of 2MP and nearly equal to that of 23DMB. These values are globally coherent with the results obtained in previous studies[1,3,4] and enable to simulate cyclic experiments under different operating conditions.

Cyclic chromatography is therefore an interesting method to characterize diffusion of very slow diffusing species, which cannot be measured using classical breakthrough curves. The cycling operating conditions must however be adapted, for the accumulation of the slow molecule in the adsorbent to be significant.

Finally, the delta loadings of 3MP and 22DMB were obtained by simulation for different cycling conditions. High flow rates and high desorption times hinder the entrance of 22DMB in the adsorbent, and maximize therefore the separation efficiency.

Notation

b_j = thermodynamic Langmuir coefficient of component j (m^3/mol)
$D_{j,nc+1}$ = Maxwell-Stefan diffusion coefficient for component j (m^2/s)
D_{ij} = Maxwell-Stefan binary exchange diffusion coefficient (m^2/s)
D_m = molecular diffusion coefficient (m^2/s)
k^c = mass transfer coefficient at the surface of the crystals (m/s)
k^f = mass transfer coefficient at the surface to the pellets (m/s)
k^m = lumped mass transfer coefficient at the surface of the pellet (m/s)
L_{bed} = packed column length (m)
nc = number of components (–)
n_{cycles} = number of cycles (–)
q_j^{sat} = adsorbed phase concentration of component j at saturation (mol/m^3 of solid)
q_j = molar concentration of species j in adsorbed phase (mol/m^3 of solid)
r_c = crystal radius coordinate (m)
R_c = crystal radius (m)
R_p = pellet radius (m)
S = section of the column (m^2)
t_{ads} = adsorption step duration (s)
t_{des} = desorption step duration (s)
t_{cycle} = duration of one cycle (s)
ε_i = extra granular porosity (–)
ε_p = intra granular macroporosity (–)
$\phi_j^{f,0}$ = volume fraction of component j in the feed (–)
$\phi_j^{f,ads}$ = volume fraction of component j in the feed during the adsorption steps (–)
$\phi_j^{f,des}$ = volume fraction of component j in the feed during the desorption steps (–)
τ = tortuosity factor (–)

Literature Cited

1. Cavalcante CL Jr, Ruthven DM. Adsorption of branched and cyclic paraffins in silicalite. 2. Kinetics. *Ind Eng Chem Res.* 1995;34:185–191.
2. Zhu W, Kapteijn F, Moulijn JA. Diffusion of linear and branched C6 alkanes in silicalite-1 studied by the tapered element oscillating microbalance. *Microporous Mesoporous Mater.* 2001;47:157–171.
3. Jolimaitre E, Tayakout-Fayolle M, Jallut C, Ragil K. Determination of mass transfer and thermodynamic properties of branched paraffins in silicalite by inverse chromatography technique. *Ind Eng Chem Res.*2001;40:914–926.
4. Koriabkina AO. Diffusion of Alkanes in MFI-Type Zeolites. Ph.D. Thesis, Technische. Universiteit Eindhoven, Eindhoven, The Netherlands, 2003.
5. Dubreuil AC, Jolimaitre E, Tayakout-Fayolle M, Méthivier A. Measurement of monobranched alkane mobility in the silicalite framework in the presence of dibranched and linear molecules. *Ind Eng Chem Res.* 2008;47:2386–2390.
6. Krishna R, Van Baten JM. Diffusion of alkane mixtures in zeolites: validating the Maxwell-Stefan formulation using MD simulations. *J Phys Chem B.* 2005;109:6386–6396.
7. Lettat K, Jolimaitre E, Tayakout M, Tondeur D. Liquid phase diffusion of branched alkanes in silicalite. *AIChE J.*2011;57:319–332.
8. Krishna R. Multicomponent surface diffusion of absorbed species: a description based on the generalized Maxwell-Stefan equations. *Chem Eng Sci.* 1990;45:1779–1791.
9. Krishna R, Van Baten JM. Letter to the editor. *AIChE J.* 2010; 58:3288–3289.
10. Lettat K, Jolimaitre E, Tayakout M, Tondeur D. Reply to the letter to the editor. *AIChE J.* 2010;56:3290.
11. Tayakout-Fayolle M, Jolimaitre E, Jallut C. Consequence of structural identifiability properties on state-model formulation for linear inverse chromatography. *Chem Eng Sci.*2000;55:2945–2956.
12. Krishna R, van Baten J. Describing diffusion in microporous materials under conditions of pore saturation. *J Phys Chem C.* 2010;114: 11557–11563.
13. Villadsen J, Michelsen ML. *Solution of Differential Equation Models by Polynomial Approximation*. NJ: Prentice-Hall, Englewood Cliffs, 1978.
14. Krishna R, Calero S, Smit B. Investigation of entropy effects during sorption of mixtures of alkanes in MFI zeolite. *Chem Eng J.* 2002; 88:81–94.
15. Denayer JFM, De Meyer KMA, Martens JA, Baron GV. Molecular competition effects in liquid phase adsorption of long chain n-alkane mixtures in ZSM-5 zeolite pores. *Angew Chem Int Ed.* 2003;42: 2774–2777.
16. Chempath S, de Meyer K, Denayer JFM, Baron GV, Snurr RQ. Adsorption of alkane mixtures from liquid phase in silicalite: simulations and experiment. *Langmuir.* 2004;20:150–156.

Manuscript received Oct. 11, 2010, and final revision received May 5, 2011.